 CMES, vol.29, no.2, pp.55-62, 2008

Kinematic Analysis of Lumbar Spine Undergoing Extension and Dynamic Neural Foramina Cross Section Measurement

Yongjie Zhang[1], Boyle C. Cheng[2], Changho Oh[1], Jessica L. Spehar[2] and James Burgess[3]

Abstract: The spinal column plays a vital biomechanical role in the human body by providing structural support and facilitating motion. As degenerative changes occur in the spine, surgical treatment may be necessary in certain instances. Such treatments seek to address pain, frequently through the restriction of spinal motion. Traditional spinal implant devices are designed to restrict the motion of a functional spinal unit (FSU) but newer device designs allow for semi-constrained motion such as spinal arthroplasty devices. In this study, a sequence of fluoroscopic imaging data was recorded during the flexibility protocol with an interspinous process spacer device placed at *L2-L3*. We use image processing techniques to characterize the performance of interspinous spacers in addition to standard biomechanical methods of comparison such as range of motion (ROM). A fast marching method and the principal component analysis are developed and utilized for kinematics analysis of lumbar spine undergoing flexion extension bending and dynamic measurement of neural foramina cross section that ideally would be applicable to patient datasets. Flexion extension bending is related to the motion of leaning backward. The implanted level exhibits a major reduction in ROM (approximately 10.4% compared to the intact state in flexion extension bending) but minor change in cross sectional foramina area (about 5.61%). Effectiveness of such devices in extension bending is important from a translational medicine point of view and requires information beyond standard ROM measures alone.

Keyword: Kinematic analysis, lumbar spine, interspinous process spacer device, image processing.

1 Introduction

Degenerative ailments of the spine occur over time as the components of the spine become worn from everyday use. Frequently, the degenerative changes involve the intervertebral disc and posterior elements including the facet joints. Of particular interest is the ability to restrict motion from a posterior approach, i.e., interspinous process device implants. Interspinous process spacers may be effective in relieving symptoms due to neurogenic claudication. This approach is particularly valuable for patients that would not tolerate more invasive surgical procedures.

Spinal implant devices have been traditionally designed to restrict motion but newer generations of designs include some that preserve motion in a functional spinal unit (FSU) or only semi-constrain motion in a FSU. Interspinous spacers reduce motion particularly in extension motion and hold the spinal motion segment in an optimized position. Previous works regarding interspinous process devices have been published in the literature on the clinical efficacy of these devices. Richards et al. examined the effect of the implant on the spinal canal and neural foramina during flexion and extension bending [Richards, Majumdar et al. (2005)]. Similarly, the influence of an interspinous implant on facet loading at the implanted and nearby region during extension was studied [Wiseman, Lindsey et al. (2005)]. In 2005, Zucherman et al. studied the safety and efficacy of the X STOP interspinous implant device

[1] Department of Mechanical Engineering, Carnegie Mellon University, Pittsburgh, PA 15213
[2] Department of Neurological Surgery, University of Pittsburgh, Pittsburgh, PA 15213
[3] Department of Neurosurgery, Allegheny General Hospital, Pittsburgh, PA 15212

[Zucherman, Hsu et al. (2005)]. In 2006, Goel et al. published a paper evaluating the safety and effectiveness of the medical device prior to the actual implantation [Goel, Panjabi et al. (2006)]. Recently, research regarding whether polymethylmethacrylate (PMMA) injected into the spinous process in order to improve the spinous compression strength of patients whose bones are relatively weak had been reported [Idler, Zucherman et al. (2008)].

The recent interest in interspinous process spacers has been due in part to the relief of pain symptoms for patients when a stenotic lumbar segment is in a forward flexed position. These implants that restrict motion in extension are known to relieve the effects of intermittent neurogenic claudication. Methods of characterizing their performance must augment current characterization that are derived from fixation standards, i.e., range of motion (ROM). Developing and utilizing image processing techniques may potentially lead to better solutions for evaluating the efficacy of these devices on the ability to restrict or minimize abnormal motion. In this paper, we will utilize the fast marching method and principal component analysis to accurately characterize the performance of interspinous spacers in addition to standard biomechanical methods of comparison.

2 Anatomy Structure of Lumbar Spine

As shown in Figure 1 [Back.com], the lumbar spine refers to the lower segment of the spinal column directly below the thoracic region but directly above the sacrum. The osteoligamentous lumbar segment consists of a vertebral body, pedicles, laminae, facet joints, spinous process, and transverse processes. The lumbar spine has five lumbar vertebrae, $L1$-$L5$, and each lumbar vertebra is comprised of a vertebral body and a vertebral arch. The vertebral body is the thick oval segment of bone forming the front of the vertebral segment.

The vertebral body profile is shaped like an hourglass, thinner in the center with thicker ends and has a hard and strong outer-shell composed of cortical bone. The vertebral arch consists of 1) a pair of pedicles which are short stout transverse processes that project from the sides of the vertebral body and 2) a pair of laminae, the flat plates extending from the pedicles which together form the arch. The vertebral arch encloses the spinal canal. Facets are the joints that interconnect the vertebral arches and help with twisting motions and rotation of the spine. The surfaces of the facet joints are covered with cartilage that help the joints glide with minimal friction against one another. The spinous process projects from the joint of the two laminae and these are the ridges which can be felt along the backbone. Transverse processes extend from the junction of the pedicles and lamina.

3 Experimental Methods

Spinal implant devices are designed to either restrict motion, e.g., fusion constructs, or preserves motion in a functional spinal unit such as spinal arthroplasty devices. Recent designs have allowed new surgical intervention strategies such as interspinous process spacers. The efficacy of these devices has been established clinically due in part to the restriction or minimization of motion while unfolding ligamentous structures may lead to neural compression and ultimately disability if left to impinge upon the neural elements. Spinal biomechanics includes the study of the kinematic response of functional spinal units in response to externally applied forces and moments. Manipulations such as flexion extension bending and axial torsion are applied to spine analogs and the effects are quantified in engineering terms. This research is a well accepted means to evaluate spinal implants prior to clinical use. State of the art treatments require sound biomechanical testing and proof prior to clinical implementation.

Our experiment was carried out by using the Bose Spine Test Machine in the Spine Biomechanics Research Laboratory in University of Pittsburgh Medical Center. The Bose spine test machine includes a six axis spine test frame with automated follower load capability, submillimeter optical tracking and fluoroscopy integrated into the biomechanical test protocols. A fresh frozen cadaveric human lumbar specimen was subjected to flexion extension bending under a pure moment protocol. $L2$-$L3$ was implanted with an X-Stop

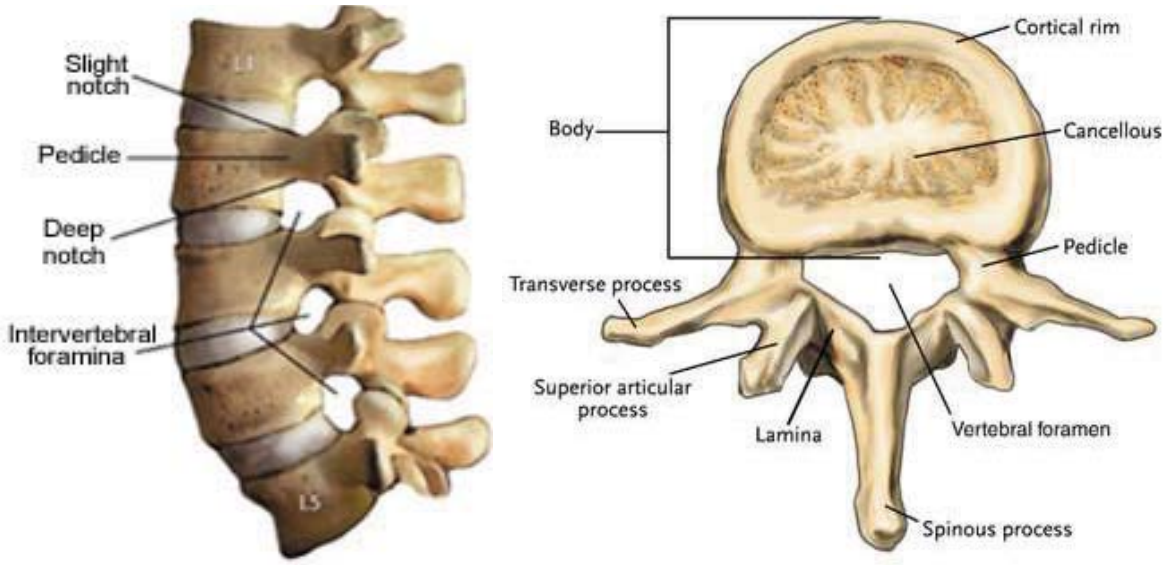

Figure 1: Anatomy of lumbar spine (`http://www.back.com/ anatomy-lumbar.html`).

interspinous spacer, which has been reported to restrict motion primarily in extension. Usually, the most common levels of degeneration of human spinal cord can be observed at *L*3-*L*4 and *L*4-*L*5 and the cadaveric specimen in this study exhibited degenerative changes at *L*3-*L*4. Thus, we chose to implant the device at *L*2-*L*3 to examine the effect of the interspinous device at a normal FSU (Functional Spinal Unit) with minimal degeneration in order to gage the effects of the device alone versus a combined effect of a potential pathological level with a device treatment. Additionally, 736 high resolution dynamic fluoroscopic images were captured and 10 images were analyzed for foramina opening area.

The post image processing technique to characterize the kinematic response of a normal and an instrumented FSU is essential in the development of clinical diagnostic tools for lumbar pathologies. Not only are such measures important in detecting changes as a result of treatment, but ideally, the early diagnosis of degenerative changes with a patient's FSU would be a significant contribution in helping clinicians identify specific problematic levels. In this study, we will use image processing techniques to characterize the performance of interspinous spacers in addition to standard biomechanical methods of comparison such as range of motion (ROM). Controlled bending protocols for flexibility testing are applied and the three dimensional kinematic response is measured.

4 Computational Methods

After acquiring the high resolution dynamic fluoroscopic images of the motion of the spine moving from flexion to extension of the third cycle, the information from the images is then analyzed for vertebral body motion and foramina cross section area based on the mean of images in the forward most flexion frames and the mean of images in the extension most frames through a fast marching algorithm and principal component analysis.

The initial phase of the study begins with segmenting the vertebral body (e.g., *L*3) and the foramina area (e.g., the foramina region between *L*2 and *L*3) in the 736 fluoroscopic images. Segmentation refers to a process to separate a digital image into multiple regions. Segmentation is generally employed to determine objects and boundaries in images. Many segmentation techniques [Yoo (2004)] exist including Region Merging, Active Surface/Front Evolution, Markov Random Field Models, and Level Set Methods. Different segmentation methods are applied to different situations to solve the image processing issue. In a previous study by Yang et al. [Yang, Tang et

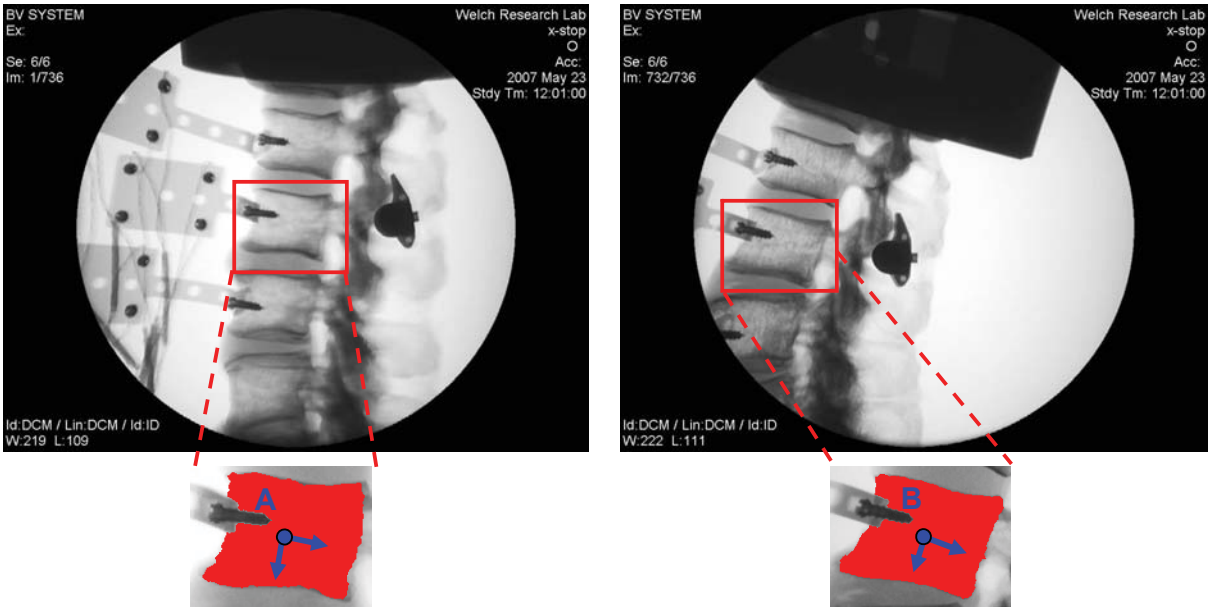

Figure 2: Segmented results of lumbar spine vertebral body L3 undergoing extension. Left – Time step 1; Right – Time step 732. Point A and B are two centroid points, and blue arrows represent two principle directions of the segmented regions (red ones).

al. (2007)], a software package of Atherosclerotic Plaque Imaging Analysis (APIA) was used to perform the segmentation of MRI images of human carotid atherosclerotic plaques. Level Set Method has also been employed to optimize topology [Wang, Lim et al. (2007); Wang, Lim et al. (2007); Wang, Lim et al. (2007)].

In this project, we choose the fast marching method [Malladi and Sethian (1998); Sethian (1999); Yu and Bajaj (2005)]. Seed points are selected in the regions of interest (e.g., the vertebral body $L3$ and its background which is the complementary region of $L3$ in Figure 2), and a contour is initialized and allowed to grow until a certain stopping condition is reached (e.g., when the boundaries of neighboring regions meet together, we stop the iteration). Every voxel is assigned with a value called time and denoted by T, which is initially zero for all the seed points and infinite for all other voxels. Repeatedly, the voxel on the marching contour with minimal time value is deleted from the contour and the time values of its neighbors are updated. The gradient of arrival time is inversely proportional to the growing speed of the isocontour, therefore the time function T satisfies the following equation:

$$\|\nabla T(x,y)\| \bullet F(x,y) = 1, \tag{1}$$

where $F(x,y) = e^{-\alpha\|\nabla I\|}$ is the speed function determined by the gradients of the input maps I ($\alpha > 0$). The resulting segmentation of the vertebral body $L3$ at time step 1 and 732 are shown in Figure 2.

If the i^{th} red pixel in this segmented image has coordinates a_i (represented as row vector), we can estimate the center and orientation of the segmented image using the principal component analysis. The centroid c of the segmented region has coordinates $\frac{1}{n}\sum_{i=1}^{n} a_i$, where n is the number of red pixels. To estimate the orientation of the segmented region, we next form the 2×2 covariance matrix M:

$$M = \frac{1}{n}\sum_{i=1}^{n}(a_i - c)^T (a_i - c). \tag{2}$$

The two eigenvectors of M are orthogonal, and they describe the directions of the first and second principal variation of the data points. Together with the centroid c, these axes represent a coordinate system for the segmented image. Figure 2

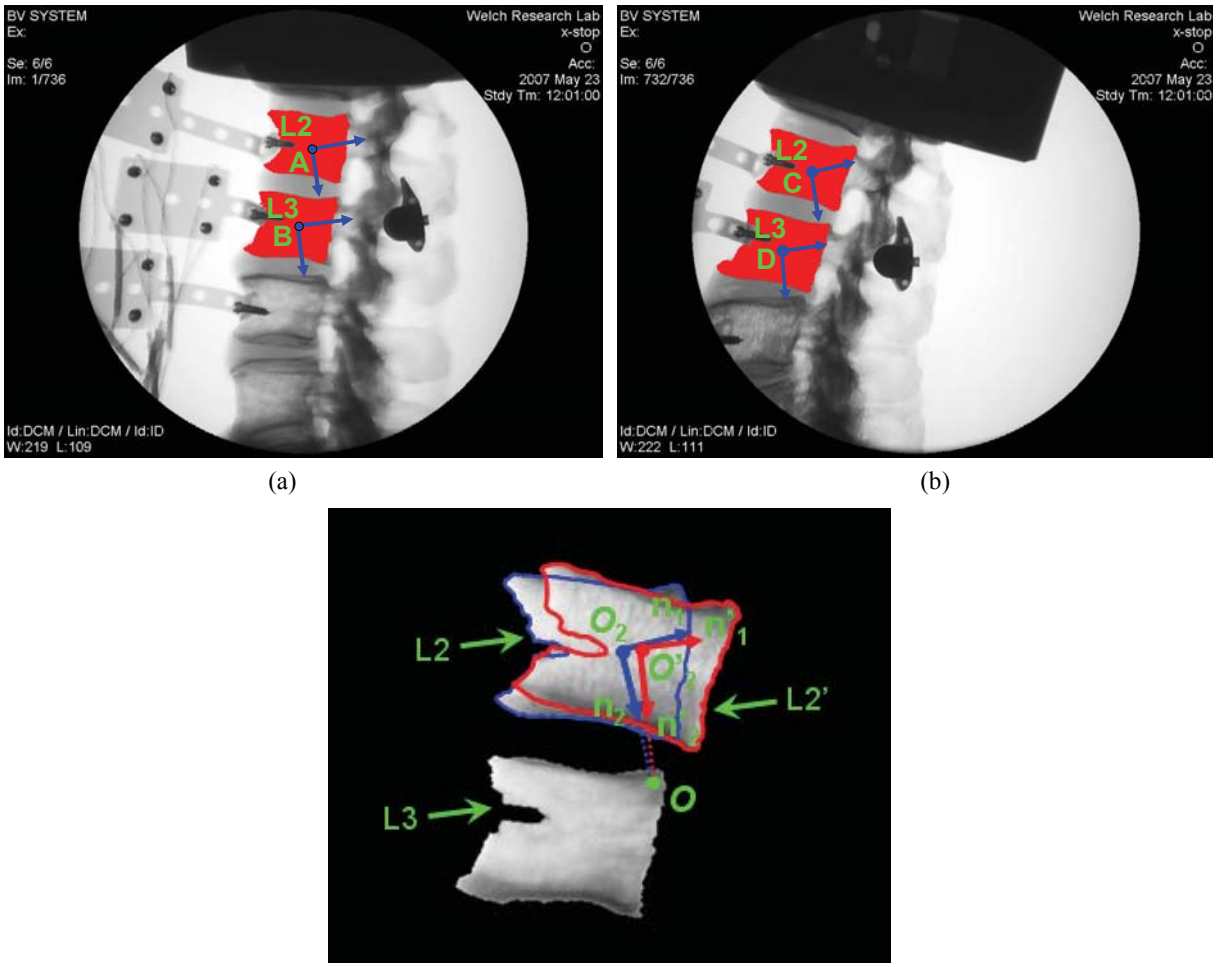

(a) (b)

(c)

Figure 3: The instantaneous rotation center. (a): Segmentation results of $L2$ and $L3$ at time step 1, (b): Segmentation results of $L2$ and $L3$ at time step 732, (c): Segmented $L2$ and $L3$ at time step 1. $L2$' is the transformation result of $L2$ from time step 732 back to time step 1. Arrows in the pictures represent the principle directions. Point A, B, C, D are the mass centers of segmented areas. Point O represents the calculated instantaneous rotation center of $L2$ relative to $L3$.

shows the calculated results of the centroids and two principle directions of $L3$ before/after extension.

The instantaneous rotation center is an important parameter for kinematic analysis of lumbar spine undergoing extension. In Figure 3, the centroid points and two principal directions are calculated for the segmented $L2$ and $L3$ at time step 1 and time step 732. By using the segmented results of $L3$ at the two time steps, we can construct an affine transformation matrix which is used to transform the segmented $L2$ at time step 732 back to time step 1, and then we obtain $L2$'. The mass centers and the two principle directions are (O_2, n_1, n_2) for $L2$ at time step 1, and (O_2', n_1', n_2') for $L2$'. The instantaneous rotation center O can be calculated from the following equation:

$$\begin{cases} \overrightarrow{OO_2} \cdot n_1 &= 0, \\ \overrightarrow{OO_2'} \cdot n_1' &= 0. \end{cases} \tag{3}$$

Figure 4 shows the resulting segmentation of the foramina cross sections between $L2$ and $L3$ at time step 1 and 732. The second phase of the study examines the area change during the flexion

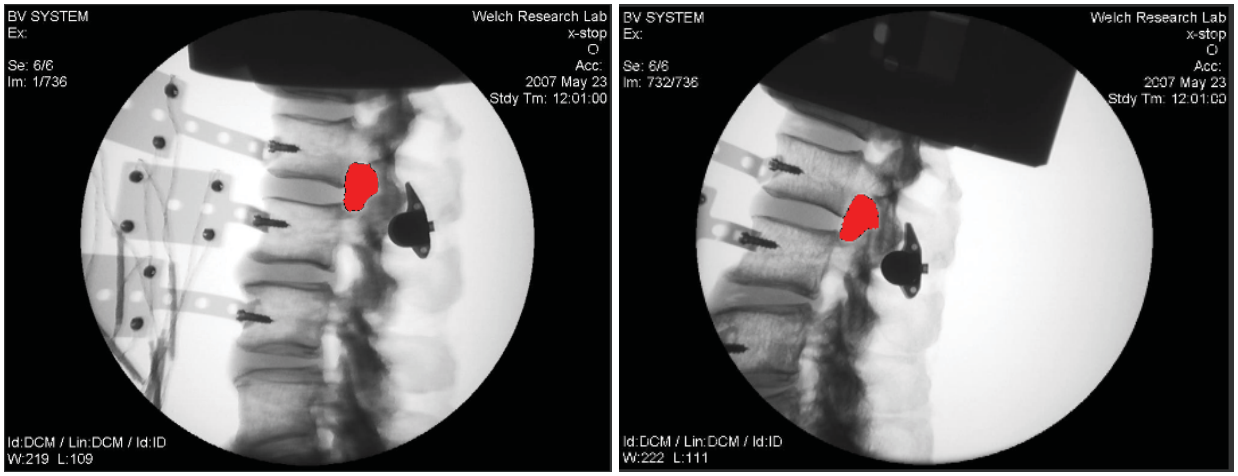

Figure 4: Segmented results (red regions) of the foramina cross sections between $L2$ and $L3$ at time step 1 (left) and time step 732 (right).

Table 1: Translation and rotation angle of $L2$ and $L3$ before/after extension

	Time Step	Centroid [mm]	$\cos^{-1}\left(\frac{\vec{n}_1 \bullet \vec{j}}{\|\vec{n}_1 \bullet \vec{j}\|}\right)$	Translation [mm]	Rotation Angle
$L2$	Time step 1 (before extension)	(122.04, 53.53)	-72.49°	(-45.43, 9.36)	-2.17°
	Time step 732 (after extension)	(76.61, 62.89)	-74.66°		
$L3$	Time step 1 (before extension)	(116.33, 85.19)	78.14°	(-50.96, 9.01)	0.74°
	Time step 732 (after extension)	(65.43, 95.24)	78.89°		

extension bending. Suppose n is the number of red pixels inside the segmented foramina region, then the foramina area is defined as $n \times \Delta x \times \Delta y$, where Δx and Δy are spacing of the imaging data along the x and y directions.

5 Results and Discussion

Suppose the top left of the image is the origin of the coordinate system, and the spacing is 0.236mm×0.225mm. Table 1 shows the translations and the rotation angles for $L2$ and $L3$ after applying flexion extension bending. The instantaneous rotational center of $L2$ relative to $L3$ from time step 1 to time step 732 is (127.56, 76.22). Table 2 shows the area change of the foramina between $L2$ and $L3$ and the area difference of the foramina between $L3$ and $L4$. We observed that the flexion extension bending results in a reduced ROM corresponding to 10.4% of the ROM found in the control. The difference in foramina cross sectional area between $L3$ and $L4$ measures 13.77%, while the area change between $L2$ and $L3$ is restricted as 5.61% since an interspinous process spacer device was implanted at $L2$-$L3$. Our experimental result can be used to validate the medical device in extension bending and locate the optimized position for the implant with the inferior adjacent level serving as a control.

ROM comparisons have been accurate in predicting the clinical efficacy of fixation hardware. However, the ability to maintain the foramina space under load has not currently been a priority to characterize. Interspinous process spacers, along with other motion preservation devices, re-

Table 2: Foramina area change at $L2-L3$ and $L3-L4$

	Time Step	Foramina Area [mm^2]	Area Change
between $L2$, $L3$	Time step 1 (before extension)	182.434	5.61%
	Time step 732 (after extension)	172.207	
between $L3$, $L4$	Time step 1 (before extension)	131.992	13.77%
	Time step 732 (after extension)	116.012	

quire additional biomechanical parameters in order to characterize clinical behavior. The implanted level exhibits a major reduction in ROM but minor change in cross sectional foramina area between the two extremes. Effectiveness of such devices in extension bending is important from a translational medicine point of view and requires information beyond ROM measures alone.

Acknowledgement: This research was supported by Carnegie Mellon University's Summer Undergraduate Research Fellowship (SURF) and a contract from University of Pittsburgh.

References

Back.com, `http://www.back.com/anatomy.html`.

Goel, V. K.; M. M. Panjabi; Patwardhan, A. G.; Dooris, A. P.; Serhan H. (2006): Test Protocols for Evaluation of Spinal Implant. *The Journal of Bone and Joint Surgery*, vol. 88-A, pp. 103-109.

Idler, C. I.; Zucherman, J. F.; Yerby, S.; Hsu, K. Y.; Hannibal, M.; Kondrashov, D. (2008): A Novel Technique of Intra-Spinous Process Injection of PMMA to Augment the Strength of an Inter-Spinous Process Device Such as the X STOP. *Spine* vol. 33, pp. 452-456.

Malladi, R.; Sethian, J. A. (1998): A real-time algorithm for medical shape recovery. *International Conference on Computer Vision*, pp. 304-310.

Richards, J. C.; Majumdar, S.; Lindsey, D. P.; Beapre, G. S.; Yerby S. A. (2005): The Treatment Mechanism of an Interspinous Process Implant for Lumbar Neurogenic Intermittent Claudication. *Spine*, vol. 30(7), pp. 744-749.

Sethian, J. A. (1999): *Level Set Methods and Fast Marching Methods*, Cambridge University Press.

Wang, S. Y.; Lim, K. M.; Khoo, B. C.; Wang, M. Y. (2007): A Geometric Deformation Constrained Level Set Method for Structural Shape and Topology Optimization. *CMES: Computer Modeling in Engineering & Sciences*, vol. 18, pp. 155-181.

Wang, S. Y.; Lim, K. M.; Khoo, B. C.; Wang, M. Y. (2007): On Hole Nucleation in Topology Optimization Using the Level Set Methods. *CMES: Computer Modeling in Engineering & Sciences*, vol. 21, pp. 219-237.

Wang, S. Y.; Lim, K. M.; Khoo, B. C.; Wang, M. Y. (2007): An Unconditionally Time-Stable Level Set Method and Its Application to Shape and Topology Optimization.*CMES: Computer Modeling in Engineering & Sciences*, vol. 21, pp. 1-40.

Wiseman, C. M.; Lindsey, D. P.; Fredrick, A. D.; Yerby, S. A. (2005): The Effect of an Interspinous Process Implant on Facet Loading During Extension. *Spine*, vol. 30, pp. 903-907.

Yang, C.; Tang, D.; Yuan, C.; Hatsukami, T. S.; Zheng, J.; Woodard, P. K. (2007): In Vivo/Ex Vivo MRI-Based 3D Non-Newtonian FSI Models for Human Atherosclerotic Plaques Compared with Fluid/Wall-OnlyModels. *CMES: Computer Modeling in Engineering & Sciences*, vol. 19, pp. 233-245.

Yoo, T. S. (2004): *Insight into Images*. Wellesey, MA, A K Peters.

Yu, Z.; Bajaj, C. L. (2005). Automatic Ultrastructure Segmentation of Reconstructed Cryo-EM Maps of Icosahedral Viruses. *IEEE Transactions on Image Processing*, vol. 14(9), pp. 1324-1337.

Zucherman, J. F.; Hsu, K. Y.; Hartjen, C. A.; Mehalic, T. F.; Implicito, D. A.; Martin, M. J.; Johnson, D. R.; Skidmore, G. A.; Vessa, P. P.; Dwyer, J. W.; Puccio, S. T.; Cauthen, J. C.; Ozuna, R. M. (2005): A Multicenter, Prospec-

tive, Randomized Trial Evaluating the X STOP Interspinous Process Decompression System for the Treatment of Neurogenic Intermittent Claudication. *Spine*, vol. 30, pp. 1351-1358.